Basic Res Cardiol 101: 159 – 167 (2006)
DOI 10.1007/s00395-005-0566-z

ORIGINAL CONTRIBUTION

Sebastian Philipp
Stuart D. Critz
Lin Cui
Viktoriya Solodushko
Michael V. Cohen
James M. Downey

Localizing extracellular signal-regulated kinase (ERK) in pharmacological preconditioning's trigger pathway

Received: 8 August 2005
Returned for revision: 18 August 2005
Revision received: 13 September 2005
Accepted: 4 October 2005
Published online: 11 November 2005

S. Philipp · L. Cui · V. Solodushko
M. V. Cohen · J. M. Downey, Ph.D. (✉)
Department of Physiology
MSB 3074
University of South Alabama
College of Medicine
Mobile, AL 36688, USA
Tel.: +1-251/460-6818
Fax: +1-251/460-6464
E-Mail: jdowney@usouthal.edu

S. Philipp
Department of Cardiology
West German Heart Center Essen
University of Duisberg-Essen
Essen, Germany

St. D. Critz
Department of Cell Biology
and Neuroscience
University of South Alabama
Mobile, Alabama 36688, USA

M. V. Cohen
Departments of Physiology and Medicine
College of Medicine
University of South Alabama
Mobile, Alabama 36688, USA

Abstract Acetylcholine (ACh) and opioid receptor agonists trigger the preconditioned phenotype through sequential activation of the epidermal growth factor (EGF) receptor, phosphatidylinositol 3-kinase (PI3-K), Akt, and nitric oxide synthase (NOS), and opening of mitochondrial (mito) K_{ATP} channels with the generation of reactive oxygen species (ROS). Although extracellular signal-regulated kinase (ERK) has recently been reported to be part of this pathway, its location has not been determined. To address this issue, we administered a 5-min pulse of ACh (550 μM) prior to 30 min of ischemia in isolated rabbit hearts. It reduced infarction from 30.4 ± 2.2% of the risk zone in control hearts to 12.3 ± 2.8% and co-administration of the MEK, and, therefore, downstream ERK inhibitor U0126 abolished protection (29.1 ± 4.6% infarction) confirming ERK's involvement. MitoK_{ATP} opening was monitored in adult rabbit cardiomyocytes by measuring ROS production with MitoTracker Red. ROS production was increased by each of three G protein-coupled agonists: ACh (250 μM), bradykinin (BK) (500 nM), and the δ-opioid agonist DADLE (20 nM). Co-incubation with the MEK inhibitors U0126 (500 nM) or PD 98059 (10 μM) blocked the increased ROS production seen with all three agonists. Direct activation of its receptor by EGF increased ROS production and PD 98059 blocked that increase, thus placing ERK downstream of the EGF receptor. Desferoxamine (DFO) which opens mitoK_{ATP} through direct activation of NOS also increased ROS. PD 98059 could not block DFO-induced ROS production, placing ERK upstream of NOS. In isolated hearts, ACh caused phosphorylation of both Akt and ERK. U0126 blocked phosphorylation of ERK but not of Akt. The PI3-K inhibitor wortmannin blocked both. Together these data indicate that ERK is located between Akt and NOS.

Key words acetylcholine – bradykinin – DADLE – ERK – U0126

Introduction

Activation of G_i-coupled surface receptors, as occurs with ischemic preconditioning (IPC), protects the heart against infarction and is dependent on generation of reactive oxygen species (ROS). Occupancy of the respective surface receptors by acetylcholine (ACh), bradykinin (BK) or the δ-opioid agonist DADLE triggers entrance of the heart into the preconditioned state [5, 13, 17, 18, 22] through a complex pathway that includes, at least for ACh and opioid, transactivation of the epidermal growth factor (EGF) receptor tyrosine kinase. Triggering by all three agonists requires Src activation [2, 11, 12, 16], stim-

BRC 566

ulation of phosphatidyinositol 3-kinase (PI3-K) [12, 18], phosphorylation of Akt [13] and activation of NOS [13, 17]. This in turn leads to a stimulation of guanylyl cyclase [17]. Subsequent activation of protein kinase G (PKG) [17] leads to opening of the mitochondrial K_{ATP} channel (mitoK_{ATP}) [17, 18] which causes ROS generation [(19]. All of these signaling steps occur during the trigger phase prior to the index ischemia to put the heart into its preconditioned state.

The extracellular signal-regulated kinases (ERK1 and ERK2), members of the mitogen-activated protein kinase (MAPK) family, must be activated at reperfusion in order to realize preconditioning's protection [7, 8]. While ERKs are known to be important during reperfusion in the preconditioned heart, few investigators have looked for them in the trigger pathway described above. Recently, however, Cao et al. [2] reported that activation of ERK 1/2 was required for an opioid agonist to trigger cardioprotection. The actual position of ERK in the trigger pathway was not determined, nor was it determined whether it was required for other triggers of preconditioning such as ACh or BK. We, therefore, decided to test whether ERK activation was required for other triggers of cardioprotection and to see if we could pinpoint ERK's position in the signaling pathway with our rabbit cardiomyocyte model.

Methods

All experiments were conducted in accordance with *The Guide for the Care and Use of Laboratory Animals* [15].

Adult rabbit myocytes

The method for isolating rabbit ventricular myocytes has been described in detail [1, 17]. Briefly, New Zealand White rabbits were anesthetized with pentobarbital sodium (30 mg/kg i.v.), anticoagulated with heparin (1000 U/kg i.v.), and ventilated with 100 % oxygen. Hearts were excised, quickly mounted on a Langendorff apparatus, and retrogradely perfused with modified calcium-free Krebs-Henseleit-HEPES buffer containing collagenase (type 2, Worthington Inc., Lakewood, NJ) (200 U/ml) at 37 °C. After 15–25 min, the softened heart was minced and passed through a nylon mesh (pore diameter 200–350 μm). Viable myocytes were separated by repetitive slow-speed centrifugation and made calcium-tolerant by stepwise restoration of calcium to 1.25 mM in buffer containing 2 % bovine serum albumin. At least 20 million viable, calcium-tolerant cells were extracted per heart. Preparations were considered satisfactory if rod-shaped cells accounted for >65 % of the cells.

Immediately after the isolation and separation procedure, cells were plated on poly-d-lysine/laminin coated 24-well plates (Becton Dickinson, Bedford, MA) using creatine- (5 mM), L-carnitine- (2 mM), and taurine- (5 mM) supplemented medium 199 (CCT-medium 199) as described by Piper et al. [21] and Mitcheson et al. [14]. Penicillin (100 U/ml) and streptomycin (100 μg/ml) were added as antibiotics. Cells were stored in an incubator at 37 °C in air enriched with 5 % CO_2. A first medium change was performed after 3–4 h; afterwards cells were allowed to equilibrate for at least 18 h. Experiments were performed 1–4 days after myocyte isolation.

Experimental design

Each experiment started with a change of medium in the wells. After 10 min, the medium was removed. If the effect of a blocker (see below) was being determined, fresh medium containing that blocker was added to the cells for 10 min. Thereafter, cells were exposed to the drug being investigated or drug + blocker (according to protocol) and reduced MitoTracker Red (chloromethyl dihydro-X-rosamine) (1 μM). The reduced form of the probe is non-fluorescent, and becomes fluorescent when oxidized by ROS. The oxidized product is bound to thiol groups and proteins within mitochondria. After incubation with MitoTracker for 15 min, cells were washed with fresh MitoTracker-free CCT medium. The wash serves two purposes. First, it removes any unbound and, thus, voltage-dependent pool of oxidized MitoTracker Red held in the cell [10]. Second, it removes unreacted reduced MitoTracker Red to stop the reaction. After washing, all that remains is the protein-bound fluorescent product, and that fluorescence is stable for at least 30 min.

The effects of the agonists BK (500 nM), ACh (250 μM), DADLE (20 nM), desferoxamine (DFO) (1 mM), and EGF (1 μg/ml) on ROS production by isolated cardiomyocytes were investigated. Two blockers of MEK, and, therefore, of downstream ERK were used: PD 98059 (10 μM) and U0126 (500 nM). Previous investigations have documented that the described protocol of a timed incubation followed by washing permits reliable measurement of ROS generation and is insensitive to changes in mitochondrial transmembrane potential [10, 16].

Measurement of ROS production

Experiments were designed such that four different conditions were always simultaneously evaluated. In each field, rod-shaped cells were considered viable, while those that were round were considered dead. Mitochondrial ROS generation was analyzed by measuring the fluorescence of at least 25–50 individual rod-shaped cells

that were randomly selected within each well. The average fluorescence of 150–300 cells was computed and expressed as a percentage of the average single cell fluorescence in the respective control well in the same chamber. Thus, treated cells were compared only to contemporary untreated cells of the same age and isolation and stained with the same MitoTracker preparation. The fluorescence of single cells was quantified as described previously [16] using a Nikon TMS-F microscope with a 20× objective, an XF filter set (Omega Optical, Brattleboro, VT), a xenon light source with a lambda 10-2 optical filter changer (excitation, 560 nm; emission, 610 nm; light source, 0.1 s; Sutter Instruments, Novato, San Diego, CA), and software from Intracellular Imaging (Cincinnati, OH). Each set of experiments was repeated on different days with cells of different ages and from at least two different isolations.

Isolated rabbit heart model

New Zealand White rabbits of either sex were anesthetized with sodium pentobarbital (30 mg/kg iv). A tracheotomy was performed, and the rabbits were mechanically ventilated with 100% oxygen using a positive-pressure ventilator at a rate of 30–35 breaths/min. A left thoracotomy was performed in the fourth intercostal space and the pericardium was opened to expose the heart. As previously described [3], a 2-0 silk suture was passed around a branch of the left coronary artery and the ends of the thread passed through a small vinyl tube to form a snare. Hearts were rapidly removed, mounted on a Langendorff apparatus by the aortic root, and perfused with modified Krebs-Henseleit bicarbonate buffer containing (mM): NaCl 118.5, $NaHCO_3$ 25, KCl 4.7, $MgSO_4$ 1.2, KH_2PO_4 1.2, $CaCl_2$ 2.5, glucose 10.0. The buffer was bubbled with 95%O_2–5%CO_2 to a pH of 7.40 (7.35–7.45) and was maintained at a temperature of 37 °C. Perfusion pressure was set at 75 mmHg. A fluid-filled latex balloon connected to a pressure transducer (Cobe) was inserted into the left ventricle and inflated to set an end-diastolic pressure of 5 mmHg. Total coronary flow was quantified by a timed collection of the perfusate exiting the right heart. All hearts were allowed to equilibrate for 20 min before the protocols were started.

Four groups of hearts were studied. All hearts were subjected to 30 min of regional ischemia and 120 min of reperfusion. Control hearts received no treatment (n = 8). The second group of hearts (n = 6) was treated with ACh (0.55 mM) for 5 min followed by 10 min of washout before the index ischemia. A third group (n = 6) was also treated with ACh. In addition, U0126 (500 nM) was added to the perfusate for 15 min starting 5 min before and ending 5 min after ACh treatment. This protocol allowed 5 min of washout before coronary occlusion. A fourth group of hearts (n = 4) was treated with U0126 with the same schedule as group 3. If required, hearts treated with ACh were electrically paced until the onset of ischemia to prevent slowing of the heart below 150 bpm.

Infarct size measurement

As previously detailed [3], the coronary artery was reoccluded and risk zone delineated as the tissue without fluorescence with 2–9 μm diameter green fluorescent microspheres (Duke Scientific Corp., Palo Alto, CA) injected into the perfusate to demarcate the risk zone as the area of tissue without fluorescence (region at risk). The hearts were weighed, frozen, and then cut into 2-mm-thick slices. The slices were incubated in 1% triphenyltetrazolium chloride (TTC) in sodium phosphate buffer (pH 7.4) at 37°C for 8 min. TTC stains noninfarcted myocardium brick red, indicating the presence of dehydrogenase enzymes in viable tissue. The slices were then immersed in 10% formalin to enhance the contrast between stained (viable) and unstained (necrotic) tissue. The areas of infarct and risk zone for each slice were determined by planimetry and volumes calculated by multiplying each area by slice thickness. These were then summed for each heart. Infarct size was expressed as a percentage of the risk zone.

Biochemical studies

Three groups of hearts were used for biochemical studies. After an equilibration time of 30 min, the first was treated with ACh (0.55 mM) alone for 5 min, while in the second an infusion of U0126 was commenced 5 min before ACh and continued for the duration of the study. In a third group, wortmannin was given as an antagonist in the same manner as U0126. In none of these hearts was ischemia induced. Excised hearts were mounted on a Langendorff apparatus and perfused with buffer. Transmural left ventricular biopsies weighing approximately 25 mg were obtained with a motorized biopsy tool. Serial tissue samples were obtained at: (1) baseline, (2) after 5 min of ACh, and (3) 10 min after the end of the ACh infusion. When blockers (U0126 and wortmannin) were given, they were continued until the last biopsy was completed. The samples were ejected into liquid nitrogen within 1 s of excision.

Tissues were prepared as previously described [12]. Electrophoresis of supernatant on 10% SDS-polyacrylamide gel was followed by transfer to a nitrocellulose membrane. Samples were assayed for phosphorylated Akt, a downstream product of activation of PI3-K, and phosphorylated ERK 1/2 with appropriate antibodies followed by incubation with secondary antibodies conjugated to horseradish peroxidase. Immunoreactive proteins were detected by enhanced chemiluminiscence with

Table 1 Hemodynamic data

Group	Baseline HR beats/min	DP mmHg	CF ml•min^{-1}•g^{-1}	Treatment HR beats/min	DP mmHg	CF ml•min^{-1}•g^{-1}	30-min occlusion HR beats/min	DP mmHg	CF ml•min^{-1}•g^{-1}	30-min reperfusion HR beats/min	DP mmHg	CF ml•min^{-1}•g^{-1}
Control	202 ± 5	113 ± 3	8.9 ± 0.3				192 ± 6	40 ± 3*	3.9 ± 0.4*	193 ± 6	76 ± 4*	6.4 ± 0.4*
ACh	218 ± 8	113 ± 2	9.4 ± 0.3	203 ± 3[1]	70 ± 15[1]	5.9 ± 1.2[1]	203 ± 3[1]	44 ± 6*	3.5 ± 0.5*	203 ± 3[1]	73 ± 4[1]	5.3 ± 0.5[1]
ACh + U0126	225 ± 8	114 ± 7	10.5 ± 0.6	217 ± 3	95 ± 11	8.6 ± 0.8[1]	220 ± 0	72 ± 6*	3.1 ± 0.1*	220 ± 0	64 ± 9*	4.4 ± 0.4*
U0126	233 ± 16	125 ± 0	9.2 ± 0.7	233 ± 13	104 ± 9	7.8 ± 0.8	215 ± 13	58 ± 9*	4.5 ± 0.5*	203 ± 9	78 ± 6*	5.8 ± 0.7[1]

Values are mean ± SEM
CF coronary flow; *DFO* desferoxamine; *DP* developed pressure; *HR* heart rate.
Statistical significance of difference between experimental observation and baseline: *$p < 0.001$, [1]$p < 0.05$

Lumi GLO. Band densities were determined with Sigmagel software. To correct for differences in protein loading and errors introduced during the transfer process, a standard myocardial sample was applied to each gel, and all band densities were normalized to this standard band and finally expressed as a percentage of that in the baseline sample.

Chemicals

All drugs required for cell isolation and culture were purchased from Sigma Chemical (St. Louis, MO). Reduced MitoTracker Red was purchased from Molecular Probes (Eugene, OR). ACh, BK, DADLE, DFO, EGF, PD 98059 and wortmannin were obtained from Sigma, and U0126 from LC Laboratories (Woburn, MA). Distilled water or DMSO was used to dissolve the drugs and prepare stock solutions. The final DMSO concentration was < 0.5%.

Phospho-Akt antibody to Ser 473 (#4051) and Thr 308 (#9275), cell lysis buffer, and Lumi GLO were purchased from Cell Signaling Technology (Beverly, MA), monoclonal anti-phospho-ERK 1/2 (#05-481) from Upstate (Lake Placid, NY), and HRP-linked anti-mouse IgG antibody from Santa Cruz Biotechnology (Santa Cruz, CA).

Data analysis

Fluorescence measurements provide data in arbitrary units (au). To remove the variability caused by different MitoTracker lots, cell age, and environmental conditions, average cell fluorescence was calculated and compared to that of simultaneously studied control cells as described above. Therefore, fluorescence data for each experiment are provided as a percentage of the control (mean ± SEM). To further minimize the possible influence of these variables on the data, ANOVA for repeated measures with Tukey's post hoc testing was used to evaluate differences in mean fluorescence of the groups within the same experiment. Baseline hemodynamic variables and risk zone and infarct size data amongst groups were compared by one-way ANOVA with Tukey's post hoc testing. Changes in serial measurements of hemodynamics for any given group were analyzed by ANOVA for repeated measures with Tukey's post hoc testing. To determine the significance of changes in phosphorylated Akt and ERK, ANOVA for repeated measures with Tukey's post hoc testing was used. A value of $p < 0.05$ was considered significant.

Results

Isolated rabbit hearts

We first attempted to extend the observation of Cao et al. [2] to see if ERK was present in ACh's trigger pathway in our infarct size model. Table 1 summarizes the serial hemodynamic data for the hearts used in the infarct size experiments. There were no differences at baseline between any of the groups. As expected, ACh depressed heart rate, developed pressure, and coronary flow during the 5-min infusion period. All of these cardiovascular measurements recovered fully during the 10-min

Table 2 Infarct data

Group	n	Body weight kg	Heart weight g	Risk zone cm^3	Infarct zone cm^3	I/R %
Control	8	2.4 ± 0.2	7.4 ± 0.6	1.35 ± 0.09	0.40 ± 0.03	30.4 ± 2.2
ACh	6	2.1 ± 0.1	7.4 ± 0.2	1.14 ± 0.09	0.14 ± 0.03*	12.3 ± 2.8*
ACh + U0126	6	1.8 ± 0.1*	5.8 ± 0.1	1.08 ± 0.10	0.30 ± 0.04	29.1 ± 4.6
U0126	4	2.2 ± 0.3	7.5 ± 0.3	1.29 ± 0.06	0.44 ± 0.07	33.8 ± 3.4

Values are mean ± SEM.
I/R ratio of infarct volume to risk zone volume; *n* number of animals.
Statistical significance of difference between experimental group and Control: *$p < 0.01$

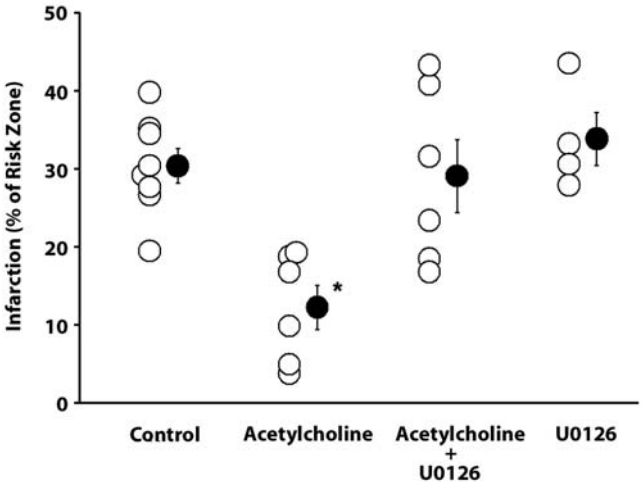

Fig. 1 The vertical axis is infarct size as a percentage of the risk zone. Open circles represent individual hearts, while closed circles indicate group means with superimposed standard errors. ACh significantly decreased infarct size, and this salutary effect was blocked by the MEK/ERK inhibitor U0126. U0126 alone did not affect infarct size. *p < 0.01

washout period. Left ventricular developed pressure and coronary flow fell further during coronary occlusion with a rebound during reperfusion. Infusion of U0126 had only a mild effect on hemodynamic variables. Table 2 contains the infarct size data. There were no differences in risk zone volume in the four groups. Infarction in control hearts averaged 30.4 ± 2.2% of risk zone (Fig. 1). A 5-min pulse of ACh prior to ischemia salvaged ischemic tissue and reduced infarct size to 12.3 ± 2.8% (p = 0.003) of the risk zone. However, this protection was abolished when the ACh infusion was bracketed with a simultaneous infusion of U0126 (29.1 ± 4.6%, p = ns). U0126 by itself had no independent effect on infarct size (33.8 ± 3.4%, p = ns).

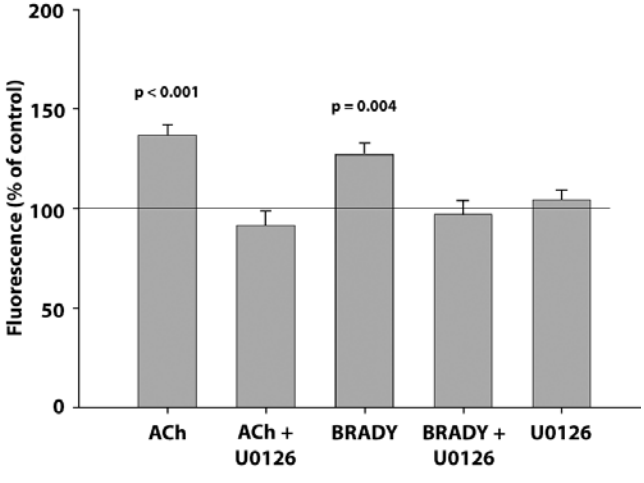

Fig. 2 Effect of acetylcholine (ACH, 250 μM) and bradykinin (BRADY, 500 nM) on generation of reactive oxygen species (ROS) in isolated rabbit cardiomyocytes. Co-treatment with the ERK inhibitor U0126 (500 nM) completely abolished this increase, whereas the inhibitor alone had no effect. Data are presented as change in fluorescence (means ± SEM) expressed as % of that of simultaneously untreated control myocytes

Isolated cardiomyocytes

BK, ACh and DADLE signaling depend on ERK activation

To further study ERK's role in the trigger pathway, we used our cardiomyocyte model in which mitoK_{ATP} opening is detected by the resulting increased ROS production. Two different MEK/ERK inhibitors were used, U0126 and PD 98059, to test whether ROS generation caused by BK, ACh, and DADLE is dependent on activation of ERK. Exposing cardiomyocytes to either ACh or BK led to robust production of ROS in cardiomyocytes as indicated by the increase in fluorescence [42 ± 7% (p < 0.001) and 27 ± 5% (p = 0.004), respectively] (Fig. 2). Co-incubation with U0126 completely blocked ROS generation from either ACh or BK.

The δ-opioid agonist DADLE also led to a significant increase in fluorescence (43 ± 5%, p < 0.001) and, therefore, ROS production in cardiomyocytes (Fig. 3). Co-incubation with U0126 prevented DADLE's effect on ROS generation. Inhibition of ERK with a second upstream MEK inhibitor, PD 98059, also blocked DADLE-induced ROS generation. Neither U0126 nor PD 98059 alone had any impact on ROS formation.

Localization of ERK in the signaling pathway

We have demonstrated that ACh-induced ROS generation in myocytes involves tyrosine phosphorylation

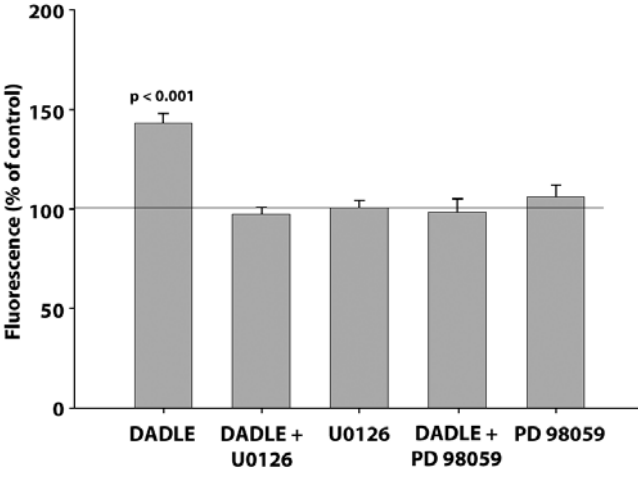

Fig. 3 Exposure of isolated cardiomyocytes to the δ-opioid agonist DADLE significantly increased ROS production, and this increase was aborted by the MEK/ERK inhibitors U0126 and PD 98059. Neither inhibitor had an effect on ROS generation

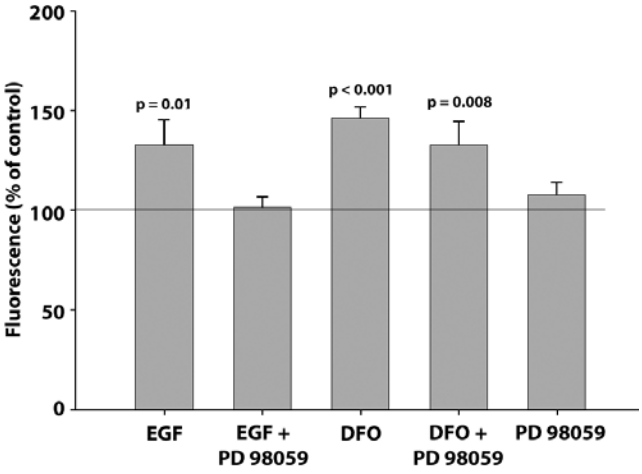

Fig. 4 Direct activation of the epidermal growth factor receptor (EGFR) with exogenous EGF caused a significant increase in ROS generation. This effect was completely blocked by PD 98059. Desferoxamine (DFO)-dependent ROS generation was not affected by co-incubation with PD 98059

(transactivation) of EGF receptors (EGFR) [11, 12]. Transactivation of the EGFR is known to activate PI3-K [11]. Figure 4 reveals that exposure of adult rabbit cardiomyocytes to exogenous EGF increased ROS generation by 33 ± 12% ($p = 0.01$) and that increase in ROS was abolished by PD 98059 (2 ± 5%, p = ns). This puts ERK downstream of the EGFR.

Desferoxamine (DFO) also generates ROS by opening mitoK_{ATP} and does so by signaling through nitric oxide, guanylyl cyclase, and protein kinase G [20]. We have demonstrated previously that DFO activates NOS independently of PI3-K or Akt [20]. As expected, DFO increased ROS production by 46 ± 5% ($p < 0.001$) (Fig. 4). Co-incubation with PD 98059 had no effect on DFO-induced ROS generation (33 ± 11%, $p = 0.008$). Again, PD 98059 alone had no effect on ROS generation. These experiments indicate that ERK is upstream of NOS.

Biochemical studies

ERK phosphorylation after ACh

Treatment of isolated hearts with ACh for 5 min significantly increased phosphorylation of ERK 1/2 by more than 50% above baseline and it remained elevated even 10 min after ACh was washed out (Fig. 5). Administration of U0126 from 5 min prior to infusion of ACh until 10 min after its cessation completely blocked ACh-induced phosphorylation of ERK 1/2, confirming that our dosage of U0126 targeted MEK/ERK. Co-administration of the PI3-K inhibitor wortmannin also inhibited ACh-induced phosphorylation of ERK 1/2. After wortmannin treatment, phosphorylated ERK levels barely exceeded baseline levels and were significantly less than those seen with ACh treatment alone ($p = 0.001$–0.003 at 5 min and 0.047 for ERK 2 after washout). These data indicate that the ERK 1/2 kinases are located downstream of PI3-K in the signaling cascade leading to cardioprotection by the NOS-PKG pathway.

Akt phosphorylation after ACh

ACh increased phosphorylation of both Akt phosphorylation sites, Ser 473 and Thr 308 (Fig. 6). Interestingly, Ser 473 phosphorylation continued to increase even after exposure of the heart to ACh was discontinued. Co-administration of wortmannin completely blocked the ACh-induced phosphorylation of both isoforms. In fact, wortmannin greatly diminished the amount of constitutive phosphorylation. On the other hand, U0126 was inef-

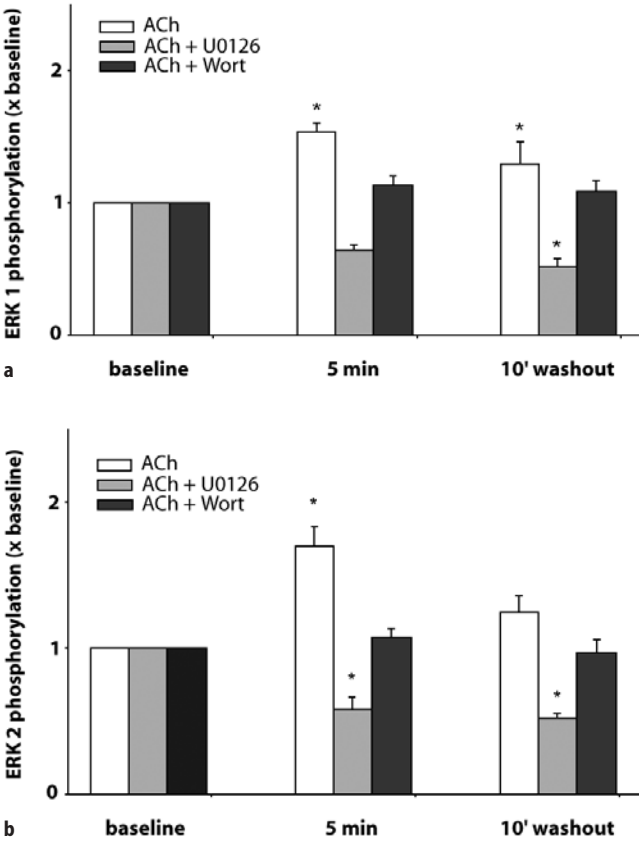

Fig. 5 Mean levels of phospho-ERK activity normalized for levels seen at baseline. Results represent mean ± SEM of five independent experiments in each of the groups. ACh (0.55 μM) was infused for 5 min. Both wortmannin and U0126 were started 5min before ACh and continued throughout the experiment. Biopsies were taken at baseline (before administration of any drug), at the end of the ACh infusion and 10 min after the end of ACh administration. ACh caused a significant increase (> 50%) of both ERK 1 (Fig. 5a) and ERK 2 (Fig. 5b) over baseline (*$p < 0.05$). However, after 10 min of washout, only the increase of ERK 1 phosphorylation remained significant. Co-administration of either U0126 (500 nM) or wortmannin (100 nM) completely blocked ACh-induced phosphorylation of ERK

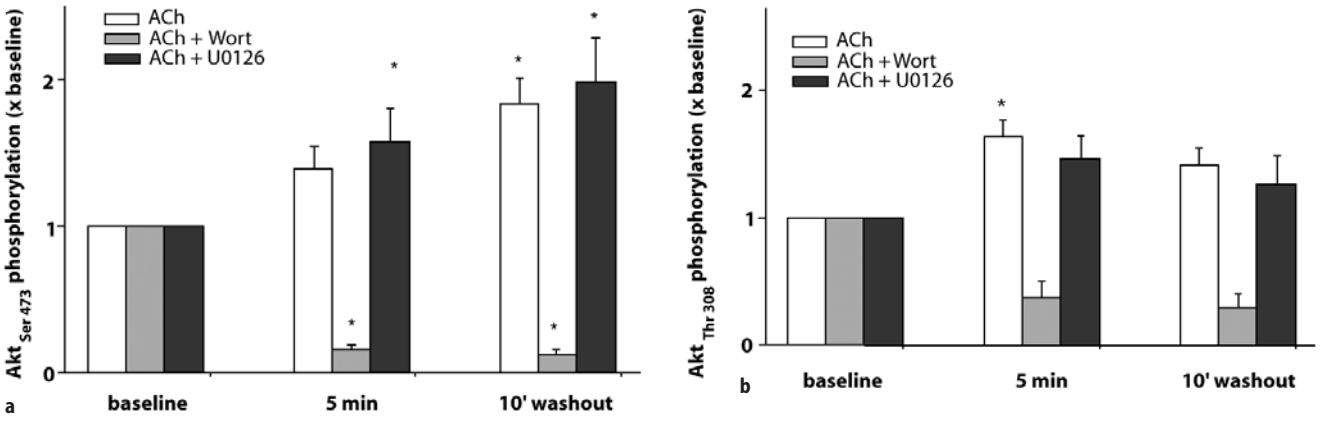

Fig. 6 Mean levels of phospho-Akt activity normalized for levels seen at baseline. Results represent mean ± SEM of at least five independent experiments for each of the groups except for four in the Thr 308 group. Drugs were infused as described in Fig. 5. ACh caused an increase in phosphorylation of both Akt phosphorylation sites, Ser 473 (Fig. 6a) and Thr 308 (Fig. 6b), above baseline, and phosphorylation at Ser 473 increased further during the washout period (*$p < 0.05$). Co-administration of wortmannin completely blocked the ACh-induced phosphorylation of both isoforms and also reduced constitutive phosphorylation. On the other hand, the ERK inhibitor U0126 did not block ACh-induced phosphorylation of Akt

fective at blocking ACh-induced phosphorylation of Akt. This is best seen for the Ser 473 site (Fig. 6a). Interestingly robust phosphorylation continued to be evident even after washout of ACh. There was no difference in the degree of Akt phosphorylation with ACh alone or the combination of ACh and U0126 at either of the two sites or the two sampling times. In the presence of U0126, ACh increased phosphorylation of Akt at Thr 308, although, presumably because of a smaller sample size, the increase was not quite significant. Because the MEK/ERK inhibitor did not affect Akt phosphorylation, we conclude that Akt resides upstream of ERK 1/2 in the signaling cascade. Taken together, all of the above results would put ERK between Akt and NOS.

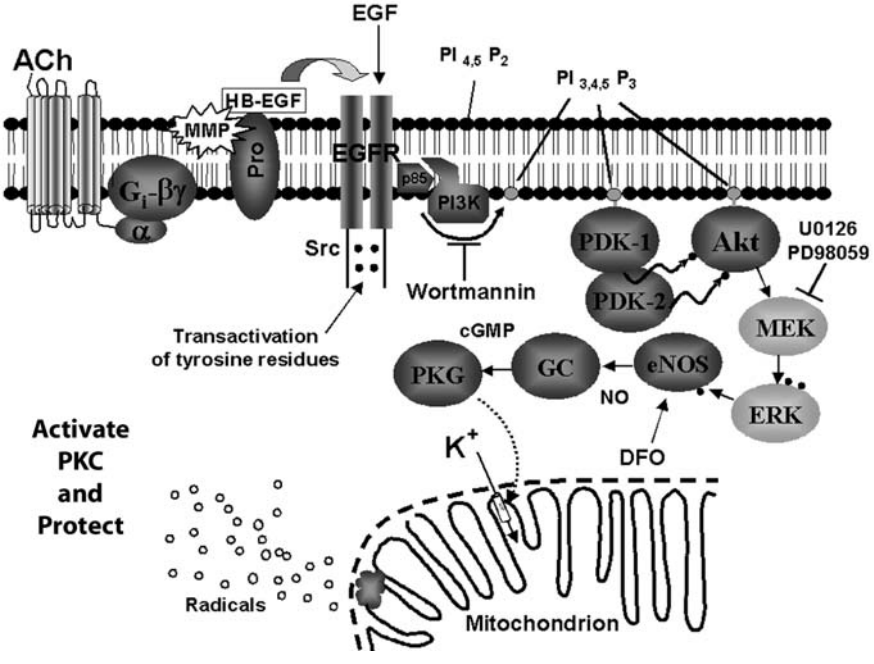

Fig. 7 Current concept of the signaling that makes up the trigger pathway of preconditioning. Acetylcholine (ACh) and other agonists of G_i-coupled receptors cause formation and release of reactive oxygen species by a complex pathway that includes the liberation of heparin-binding epidermal growth factor (EGF)-like growth factor (HB-EGF) by a metalloproteinase (MMP), transactivation of the EGF receptor (EGFR), activation of phosphatidylinositol 3-kinase (PI3K), Akt, endothelial nitric oxide synthase (eNOS), and protein kinase G (PKG) and finally opening of the mitochondrial ATP-sensitive potassium channel in that order. We now insert MAP kinase kinase (MEK) and extracellular signal-regulated kinase (ERK) between Akt and eNOS. In our experiments, PD98059 and U0126 were assumed to block MEK from phosphorylating ERK, while desferoxamine (DFO) activated eNOS directly, wortmannin blocked PI3K, and EGF populated the EGFR.
cGMP cyclic GMP; *GC* guanylyl cyclase; *PDK* phosphoinositide-dependent kinase; *PIP_2, PIP_3* phosphatidylinositol bisphosphate, trisphosphate; *PKC* protein kinase C; *Pro* pro-HB-EGF; *Src* Src kinase

Discussion

The present study reveals that activation of ERK 1/2 is required for ACh to trigger the preconditioned state in intact rabbit hearts. Because ACh is known to trigger that protection by ROS generation resulting from opening of mitoK$_{ATP}$, we monitored that opening in isolated cardiomyocytes. ACh-induced opening of mitoK$_{ATP}$ also required the activation of ERK 1/2, placing the latter somewhere between the muscarinic receptor and mitoK$_{ATP}$. Since ERK 1/2 was shown to be located upstream of NOS but downstream of the EGFR, PI3-K and Akt, one can place it between Akt and NOS.

The signal transduction pathways responsible for ischemic preconditioning have been found to be quite complex. In general, they can be divided into two categories: 1) those that are activated prior to the onset of the lethal ischemia and trigger the transition to the protected phenotype, and 2) those that are activated upon reperfusion following the lethal ischemic event and prevent death of the reperfused myocardium. We have extensively mapped the trigger pathway for many G protein-coupled receptors and generally find that it includes EGFR, PI3-K, Akt, NOS, guanylyl cyclase, PKG, mitoK$_{ATP}$ and ROS, in that order [4]. Adenosine receptors are the primary exception to that pattern and seem to bypass this entire cascade [3]. Much less is known about the pathways which protect the preconditioned heart at the time of reperfusion. Most studies have concentrated on two kinases, PI3-K and ERK 1/2 [9], and, until recently, ERK was thought to be important only at the time of reperfusion. However, Cao et al. [2] reported that the MEK inhibitors, and, therefore, effective blockers of downstream ERK, PD 98059 and U0126, could block the ability of an opioid receptor agonist to trigger protection in isolated rabbit cardiomyocytes exposed to simulated ischemia. The present study extends that observation using ACh as the trigger and the more traditional model of infarct size in an intact heart as the end-point. Other than showing that a PKC isoform resides upstream of ERK, the studies by Cao et al. included no other data that could further localize ERK in the signal transduction pathway. Based on the present study, it would now appear that ERK 1/2 is located between Akt and NOS in the trigger pathway. It is well known that ERKs are activated by EGFR, but not appreciated that they could carry an activation signal to NOS. Based on the previous report that Akt directly phosphorylates eNOS in other cell systems [6], we assumed the same was happening in cardiomyocytes. The present data indicate that additional steps including ERK activation occur between Akt and eNOS, at least in cardiomyocytes.

There are two isoforms of ERK, the 44 kD ERK1 and the 42 kD ERK 2. Both are very similar in structure and function. It is not yet known whether only one or both isoforms are involved in the signaling. Other steps such as MEK1 are also likely to be included in the pathway.

Our findings differ from those of Xu et al. [23]. The latter used isolated rat cardiomyocytes and found that the nitric oxide donor SNAP caused phosphorylation of ERK 1/2. This ERK phosphorylation could be blocked by the ROS scavenger MPG, thus placing ERK downstream of mitoK$_{ATP}$ opening. In addition, they were able to block SNAP's protection against infarction in the intact heart with PD 98059, which would again place ERK downstream of NOS. Xu et al. tested only one MEK/ERK inhibitor, namely PD 98059, to block SNAP's protection. Since ERK is known to be involved in the reperfusion phase, it is important that the inhibitor be readily washed out before the onset of ischemia if the focus is on signaling in the trigger phase. We performed two experiments (data not shown) in which we administered U0126 and then washed it out prior to infusing ACh. ACh's ability to limit infarction was not blocked in those studies indicating that the effect of U0126 is indeed reversible and that the effects we studied were indeed confined to the trigger phase. We are unaware of any comparable data for PD 98059. The ability of Xu et al. to block SNAP-induced ERK phosphorylation with MPG may well have been influenced by the additional ERK activation in the preconditioned heart during reperfusion [9]. We, on the other hand, were able to block ROS production in rabbit cardiomyocytes with both PD 98059 and U0126, clearly showing the involvement of ERK upstream of ROS.

Of course, all studies that employ pharmacological agonists and inhibitors are subject to potential nonspecific effects of the antagonist chosen. Hence, we have endeavored to use more than one inhibitor to show ERK's involvement. Nevertheless, the actual involvement of ERK and our localization of it is totally dependent on the use of pharmacological inhibitors and activators. The phosphorylation studies strengthen our conclusions, but still do not completely prove the case. Thus, further studies will be needed before ERK's exact location and role are completely understood.

In conclusion, our results indicate that, when ACh is used to induce a protected state in the rabbit heart, it activates a signal transduction pathway that includes activation of ERK 1/2 as one of its steps. The ERK 1/2 activation step occurs downstream of EGFR, PI3-K and Akt, but upstream of NOS.

Acknowledgment This study was supported in part by grants HL-20648 and HL-50688 from the Heart, Lung and Blood Institute of the National Institutes of Health. S. Philipp was supported by a grant from the Deutsches Institut für Bluthochdruckforschung, Heidelberg, Germany.

References

1. Armstrong S, Downey JM, Ganote CE (1994) Preconditioning of isolated rabbit cardiomyocytes: induction by metabolic stress and blockade by the adenosine antagonist SPT and calphostin C, a protein kinase C inhibitor. Cardiovasc Res 28:72–77
2. Cao Z, Liu L, Van Winkle DM (2005) Met^5-enkephalin-induced cardioprotection occurs via transactivation of EGFR and activation of PI3K. Am J Physiol 288: H1955–H1964
3. Cohen MV, Yang X-M, Liu GS, Heusch G, Downey JM (2001) Acetylcholine, bradykinin, opioids, and phenylephrine, but not adenosine, trigger preconditioning by generating free radicals and opening mitochondrial K_{ATP} channels. Circ Res 89:273–278
4. Critz SD, Cohen MV, Downey JM (2005) Mechanisms of acetylcholine- and bradykinin-induced preconditioning. Vascul Pharmacol 42:201–209
5. Fryer RM, Wang Y, Hsu AK, Nagase H, Gross GJ (2001) Dependence of δ_1-opioid receptor-induced cardioprotection on a tyrosine kinase-dependent but not a Src-dependent pathway. J Pharmacol Exp Ther 299:477–482
6. Fulton D, Gratton J-P, McCabe TJ, Fontana J, Fujio Y, Walsh K, Franke TF, Papapetropoulos A, Sessa WC (1999) Regulation of endothelium-derived nitric oxide production by the protein kinase Akt. Nature 399:597–601
7. Hausenloy DJ, Mocanu MM, Yellon DM (2003) Activation of the pro-survival kinases (PI3 kinase-Akt and Erk 1/2) at reperfusion is essential for preconditioning-induced protection. Circulation 108:IV–62 (Abstract)
8. Hausenloy DJ, Mocanu MM, Yellon DM (2004) Cross-talk between the survival kinases during early reperfusion: its contribution to ischemic preconditioning. Cardiovasc Res 63:305–312
9. Hausenloy DJ, Tsang A, Mocanu MM, Yellon DM (2005) Ischemic preconditioning protects by activating prosurvival kinases at reperfusion. Am J Physiol 288: H971–H976
10. Krenz M, Oldenburg O, Wimpee H, Cohen MV, Garlid KD, Critz SD, Downey JM, Benoit JN (2002) Opening of ATP-sensitive potassium channels causes generation of free radicals in vascular smooth muscle cells. Basic Res Cardiol 97:365–373
11. Krieg T, Cui L, Qin Q, Cohen MV, Downey JM (2004) Mitochondrial ROS generation following acetylcholine-induced EGF receptor transactivation requires metalloproteinase cleavage of proHB-EGF. J Mol Cell Cardiol 36: 435–443
12. Krieg T, Qin Q, McIntosh EC, Cohen MV, Downey JM (2002) ACh and adenosine activate PI3-kinase in rabbit hearts through transactivation of receptor tyrosine kinases. Am J Physiol 283: H2322–H2330
13. Krieg T, Qin Q, Philipp S, Alexeyev MF, Cohen MV, Downey JM (2004) Acetylcholine and bradykinin trigger preconditioning in the heart through a pathway that includes Akt and NOS. Am J Physiol 287:H2606–H2611
14. Mitcheson JS, Hancox JC, Levi AJ (1998) Cultured adult cardiac myocytes: future applications, culture methods, morphological and electrophysiological properties. Cardiovasc Res 39:280–300
15. National Research Council. Guide for the Care and Use of Laboratory Animals. 7th ed. 1996. Washington, D.C., National Academy Press
16. Oldenburg O, Critz SD, Cohen MV, Downey JM (2003) Acetylcholine-induced production of reactive oxygen species in adult rabbit ventricular myocytes is dependent on phosphatidylinositol 3- and Src-kinase activation and mitochondrial K_{ATP} channel opening. J Mol Cell Cardiol 35:653–660
17. Oldenburg O, Qin Q, Krieg T, Yang X-M, Philipp S, Critz SD, Cohen MV, Downey JM (2004) Bradykinin induces mitochondrial ROS generation via NO, cGMP, PKG, and mitoK_{ATP} channel opening and leads to cardioprotection. Am J Physiol 286: H468–H476
18. Oldenburg O, Qin Q, Sharma AR, Cohen MV, Downey JM, Benoit JN (2002) Acetylcholine leads to free radical production dependent on K_{ATP} channels, G_i proteins, phosphatidylinositol 3-kinase and tyrosine kinase. Cardiovasc Res 55:544–552
19. Pain T, Yang X-M, Critz SD, Yue Y, Nakano A, Liu GS, Heusch G, Cohen MV, Downey JM (2000) Opening of mitochondrial K_{ATP} channels triggers the preconditioned state by generating free radicals. Circ Res 87:460–466
20. Philipp S, Cui L, Ludolph B, Kelm M, Schulz R, Cohen MV, Downey JM (2005) Desferoxamine and ethyl-3,4-dihydroxybenzoate protect myocardium by activating NOS and generating mitochondrial ROS. Am J Physiol 290:H000–H000
21. Piper HM, Probst I, Schwartz P, Hütter FJ, Spieckermann PG (1982) Culturing of calcium stable adult cardiac myocytes. J Mol Cell Cardiol 14:397–412
22. Schulz R, Cohen MV, Behrends M, Downey JM, Heusch G (2001) Signal transduction of ischemic preconditioning. Cardiovasc Res 52:181–198
23. Xu Z, Ji X, Boysen PG (2004) Exogenous nitric oxide generates ROS and induces cardioprotection: involvement of PKG, mitochondrial K_{ATP} channels, and ERK. Am J Physiol 286: H1433-H1440